

# Theoretical and Experimental Studies on Semi-Active Smart Pin Joint

Yancheng Li, Jianchun Li, Bijan Samali

*Centre for Built Infrastructure Research, Faculty of Engineering and Information Technology,  
University of Technology Sydney, Sydney, Australia*

Jiong Wang

*School of Mechanical Engineering, Nanjing University of Science and Technology Nanjing, China*

**ABSTRACT:** An intelligent structural system equipped with smart structural members that are controllable in real-time is one effective solution to prevent structural damage and failure during hostile dynamic loadings, thereby leading to effective protection of structures and their occupants. The primary purpose of this study is to design, fabricate and characterise a prototype smart member, namely a semi-active magnetorheological (MR) pin joint, through theoretical modelling and experimental investigation. Design of prototype smart pin joints includes theoretical analysis relating to the rotary plate radius, the property of MR fluids and the gap between the rotary plate and the casing based on the requirements of the dynamics of MR pin joints. It is verified that an MR pin joint with a diameter of 180mm can produce a torque of up to 30 Nm, which is deemed adequate for realisation of the semi-active control for multi-storey building models in the next stage of research.

## 1 INTRODUCTION

Urbanisation has been and will still be a trend around the world in the 21st century. As a result, further concentration of population in big cities along coast lines makes the community and infrastructures even more vulnerable and susceptible to natural or man-made hazards. It has, therefore, been a great motivation and challenge for governments and the engineering community all over the world to find a solution for the protection of civil infrastructure and hence the community from natural or man-made hazards such as major seismic events, strong winds, sudden impact and explosion, as well as ageing, deterioration, misuse and poor quality construction (Soong T. T. 1990, Fujino, Y., Soong, T.T. & Spencer Jr., B.F. 1996).

Semi-active members such as piezoelectric (PZT) actuators (Xu Y. L. & Chen B 2008), shape memory alloy actuators (Li, J. & Samali, B 2000), MR devices (Li W. H. & Du H. 2003, Hiemenz G. J., Choi Y. T. & Wereley N. M. 2003, Widjaja J., Samali B. & Li J 2007), having advantages such as low power requirement and real-time controllability have attracted considerable attention in the last three decades. Compared with other semi-active devices, MR devices are adequate for implementation in civil structures due to the large yield stress of MR fluids (up to 60 kPa) and hence the large damping force of

MR devices. A semi-active MR pin joint, whose joint moment resistance can be controlled in real-time by altering the magnetic field, is a potential candidate for smart structural members for realization of prototype intelligent structures.

As a preliminary research aiming to the full-development of intelligent structures, the primary purpose of this study is to design, fabricate and characterise a prototype smart member, namely, a semi-active MR pin joint, through theoretical modelling and experimental investigation. This prototype smart pin using MR fluids, designed and fabricated by the NJUST engineering workshop, behaves as a free rotating hinge when not magnetised, otherwise as a partly or fully fixed joint depending on the applied magnetic field intensity levels. By real-time changing of the fixity rate of the pin, the system frequency can be altered to suit structural control requirements.

## 2 DESIGN OF MR PIN JOINT

A sketch map of a disk-type MR pin joint is shown in Figure 1. The MR pin joint mainly consists of five parts: a rotary thin plate inside the pin joint, a shaft connected to the plate to transfer the joint moment, two uniform housings to form the hollow cavity, MR fluids between the housing and plate, and a circular coil producing a magnetic field to magnetise MR fluids. There are gaps of about 1 mm between the

plate and the housings, to hold the MR fluids therein.

To achieve a saturated magnetic field in the gap, the magnetic properties of the housings, rotary plate and shaft must be carefully considered during the structural design process. MR rotary pin joints require highly magnetically permeable pole pieces for directing the magnetic flux across the working fluid gaps contained therein. In some cases there can be unwanted stray magnetic flux which can detract from the effectiveness of the device. Stray or flanking flux paths can lead to a loss of efficiency because magnetic fields and associated field energy are developed where they are not needed or desired (Carlson J. D., Leroy D. F., Holzheimer J. C., et al., 1997). This may cause remnant magnetism in any hard-magnetizable component present in the pin joint. This remnant magnetism can attract the magnetically-soft medium into areas where it may be undesirable to have it, for example, adjacent to the shaft seal.

Inside the gap is filled with MR liquid (MRF140CG) from Lord Corporation, which can provide a yield stress of up to 60kPa at saturated magnetic field. Due to the high capacity of MR fluids, this MR pin joint can produce about 30Nm with a saturated current of 2.0 A, as shown in part 4 in this paper. Other structural parameters of the pin joint are listed in Table 1.

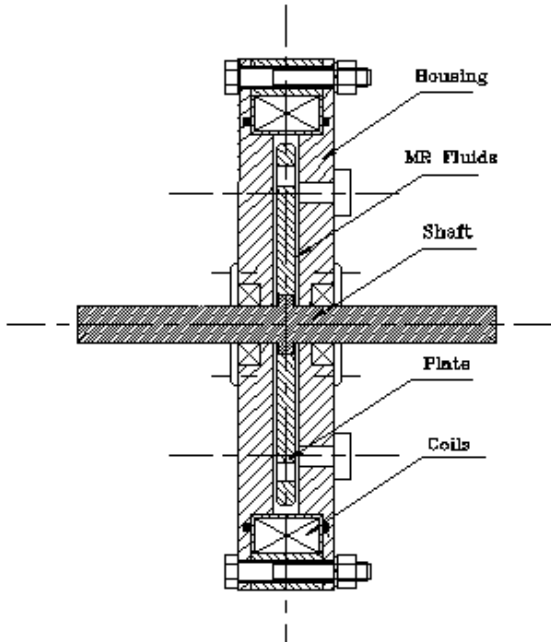


Figure 1. Sketch map of MR pin joint

Table 1. Structural parameters of the MR pin joint (mm)

Parts	Size (mm)
Shaft radius $R_1$	12.5
Radius of rotary plate $R_2$	50
Gap $h$	1
Outer diameter $D$	180
Inner diameter $d$	120
Thickness $B$	70

### 3 THEORETICAL MODELLING OF SEMI-ACTIVE MR PIN JOINT

Inside a MR pin joint, the MR fluids flow rotationally between the plate and the housing, as shown in Figure 2. Compared with the plate diameter (usually 0.5-1.0 mm), the gap between the plate and the housing is very small. Thus, the flow of MR fluids in the gap can be regarded as the flow between two parallel plates.

For any micro-body in the plate, the area of body is

$$dS = 2\pi r \cdot dr$$

$$dT = F \cdot r = (\tau \cdot dS) \cdot r = \tau \cdot 2\pi r^2 \cdot dr$$

Then the torque applied on one side of the plate is

$$T_1 = \int dT = \int_{R_1}^{R_2} \tau \cdot 2\pi r^2 \cdot dr \quad (1)$$

The Bingham plastic model which describes the dynamic behaviour of MR fluids is given by

$$\tau = \tau_y + \eta \frac{\partial u}{\partial y} \quad (2)$$

where  $\tau$  is shear stress,  $\tau_y$  is the dynamic yield stress,  $\eta$  is the fluids viscosity, and  $u$  the velocity of the plate.

In view of plate velocity expressed as a summation of rotary speed and plate radius, as

$$u = \omega \cdot r + \frac{r \cdot \omega}{h} \cdot y$$

Then

$$\frac{\partial u}{\partial y} = \frac{r \cdot \omega}{h}$$

Therefore, the total torque of the MR pin joint is

$$T = 2 \int dT = 2 \int_{R_1}^{R_2} (\tau_y + \eta \frac{R \cdot \omega}{h}) \cdot 2\pi r^2 \cdot dr$$

$$T = \frac{\pi \eta \omega}{h} (R_2^4 - R_1^4) + \frac{4}{3} \pi (R_2^3 - R_1^3) \tau_y \quad (3)$$

The torque that a MR brake produces consists of two parts:

$$T_\eta = \frac{4}{3} \pi (R_2^3 - R_1^3) \tau_y \quad (4)$$

$$T_{vis} = \frac{\pi \eta \omega}{h} (R_2^4 - R_1^4) \quad (5)$$

Where, Coulomb torque,  $\tau_\eta$ , is the torque related to the yield stress of MR fluids due to coil current; Viscosity torque,  $\tau_{vis}$ , is the torque related to the fluid viscosity.

Hence, the total torque produced by the MR pin joint is:

$$T_{total} = T_\eta + T_{vis} + T_{fri}$$

Where,  $\tau_{fri}$  is the friction torque induced by the friction between the outer housing and the shaft. It should be noted that the friction torque is very small

compared with total torque and will not be considered in theoretical analyses.

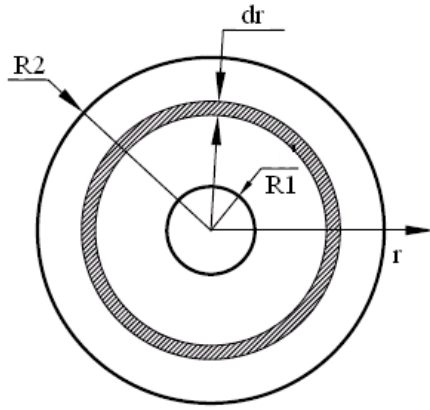


Figure 2. Rotary plate under shear stress

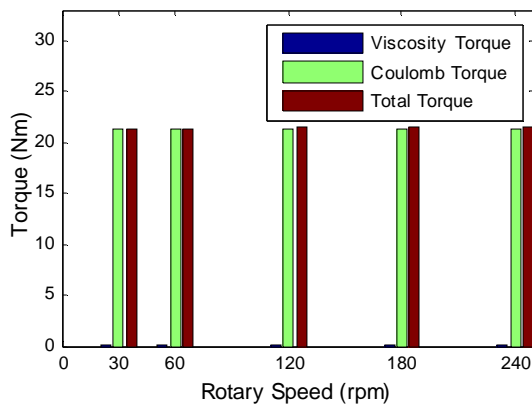


Figure 3. Distribution of viscosity torque and total torque ( $I=1A$ )

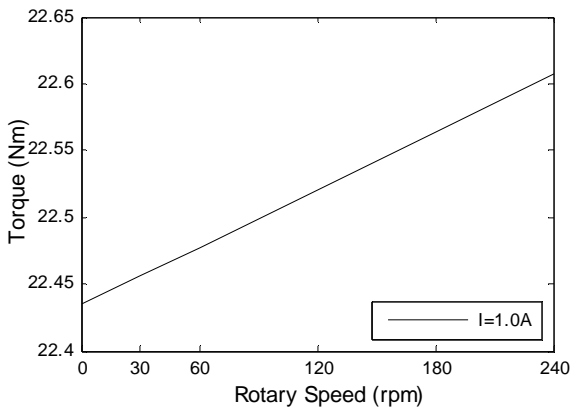


Figure 4. Impact of rotary speed on total torque

## 4 THEORETICAL ANALYSIS

### 4.1 Viscosity torque and coulomb torque

Recalling from equations (4) and (5), the overall torque includes viscosity torque  $\tau_{visi}$  and Coulomb torque  $\tau_c$ . Figure 3 indicates the distribution of these two types of torques when the coil current is 1.0A.

It is clear that the Coulomb torque is the main contribution to the total torque of the MR pin since viscosity torque is really small, e.g. when the viscosity torque is about 1Nm and Coulomb torque is more than 20 Nm. It can also be observed that the rotary speed has little influence on the total torque. The impact of rotary speed on the torque output can be numerically shown by Figure 4. With an increasing rotary speed from 0 rpm to 240 rpm, the torque is increased by only 0.171 Nm.

### 4.2 Structural parameters and torque output

To investigate the impact of structural parameters such as the gap, shaft radius and plate radius on the total torque output, numerical simulations were conducted.

Figure 5 shows the effect of gap dimension on the capacity of the MR pin joint at the current level of 2.0A. Unlike the MR damper in which the gap size is critical for its damping ability, it is of less importance in the MR pin joint. Since the gap should not be smaller than 0.5mm in reality due to increased difficulty in fabrication and operation, a relatively larger gap is acceptable in designing a MR pin joint.

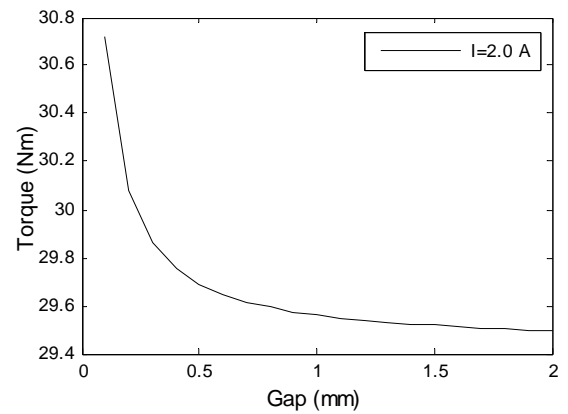


Figure 5. Impact of gap dimension on total torque

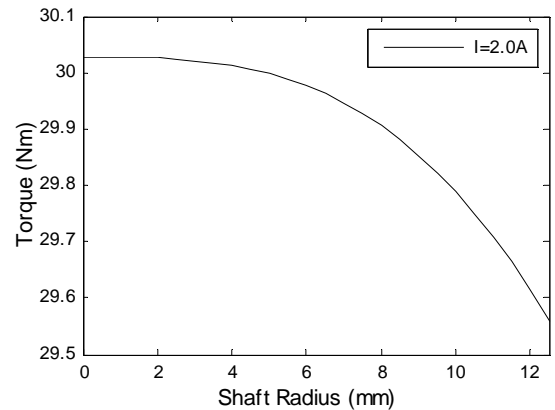


Figure 6. Impact of shaft radius on total torque

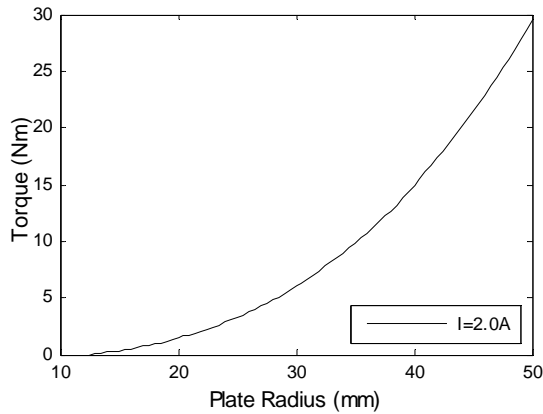


Figure 7. Impact of plate radius on total torque

The impact of shaft radius and plate radius on the torque are shown in Figures 6 and 7, respectively, based on the assumption that the structure of the designed pin joint will not be altered. The plate radius is the most important element to develop a large-torque MR pin joint according to the theoretical analysis. For example, a small plate radius less than 35 mm leads to a torque capacity of no more than 10 Nm.

## 5 EXPERIMENTAL SET-UP

To validate the design and evaluate the performance of the MR pin joint, an experiment was conducted and its set-up is as shown in Figure 8. The set-up mainly consists of four parts: an AC motor, a torque sensor, a DC power supply and the MR pin joint. The AC motor can produce a series of static rotary speeds from 0 to 500 rpm with the assistance of an adjustable frequency inverter, SA2150. A torque sensor JN338, having a capacity of 50 Nm, is used to measure the torque transmitted from the MR pin joint to the AC motor. The AC motor, torque sensor and the MR pin joint are installed in such a way that all the centroids are on the same horizontal line. A DC power supply provides the required currents to the magnetic coil in the MR pin joint. A multi-meter is connected to the DC power supply and the MR pin joint to ensure the required current.

Two connectors are implemented between the AC motor and torque sensor, and the torque sensor and the MR pin joint to transmit the torque to each other. The test rig is fixed to solid ground in order to reduce unwanted vibrations.

During the tests, all data are recorded after AC motor outputs a steady rotary speed.

## 6 EXPERIMENTAL RESULTS

MR pin joints performance under a series of rotary speeds and coil currents was experimentally investigated using the test rig shown in Figure 8. Five rota-

ry speeds, such as 30, 60, 120, 180 and 240 rpm, corresponding to the rotary frequency of 0.5, 1, 2, 3 and 4Hz, were used in the test. Moreover, five coil currents, i.e., 0, 0.5, 1.0, 1.5 and 2.0 Amp, were introduced using the DC power supply.

Figure 9 shows a plot of the transmitted torque versus the coil current at various rotary speeds of  $\omega = 30$  rpm, 60 rpm, 120 rpm, 180 rpm and 240 rpm. It can be seen from the figure that the torque is not sensitive to different rotary speeds. That is to say, coil current plays a dominant role among all the factors concerning torque output.

Figure 10 shows a series of transmitted torques versus rotary speeds at five current levels. It can be observed from Figure 11 that in the steady state output torques are nearly independent of the rotary speed. For example, with the increase of rotary speed from 30 rpm to 240 rpm at the current of 0.5A, the torque has an insignificant increase from 12.842 Nm to 13.530 Nm. Figure 10 can also validate the design, for example, the saturated current of the MR pin joint is about 2.0 Amp which is consistent with the theoretical estimation.

A comparison between the theoretical analysis and experimental results is shown in Figure 11. The distinct lag of the theoretical results to the experimental curve is due to the fact that the friction torque is not considered in the theoretical analysis. It can also be observed that a linear relationship exists between the total torque and the coil current before the saturation point.

Conclusively, both the theoretical analysis and experimental tests show that the designed MR joint possesses an ability to dramatically change the output moment resistance in a controllable manner. For example, the torque of the MR pin joint can be changed from less than 1 Nm to 30 Nm. Regardless of the rotary speed, the capacity of the MR pin joint can be easily controlled by altering the current in the magnetic coil. Possessing a small zero-field torque and large saturated torque, the designed MR pin joint can be considered a good candidate for smart members to realise the concept of intelligent structures.

## 7 CONCLUSIONS

As a preliminary study aimed to develop an intelligent civil structure equipped with smart structural members, such as a semi-active MR pin joint, this research focused on design, fabrication and testing of MR pin joints. The investigations included theoretical analysis and experimental validation. It was found that the proposed MR pin joints, with a diameter of 180 mm, has the capability to produce adjustable torques from less than 1 Nm to 30 Nm by simply altering the coil current. It makes such a pin joint to become a strong candidate as a smart member for the development of an intelligent structure.

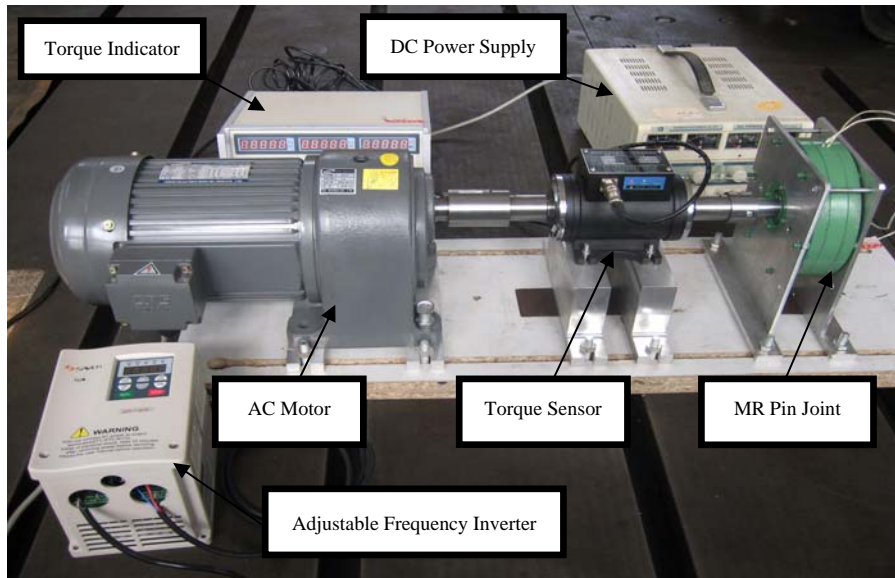


Figure 8 Experimental set-up of MR pin joint test

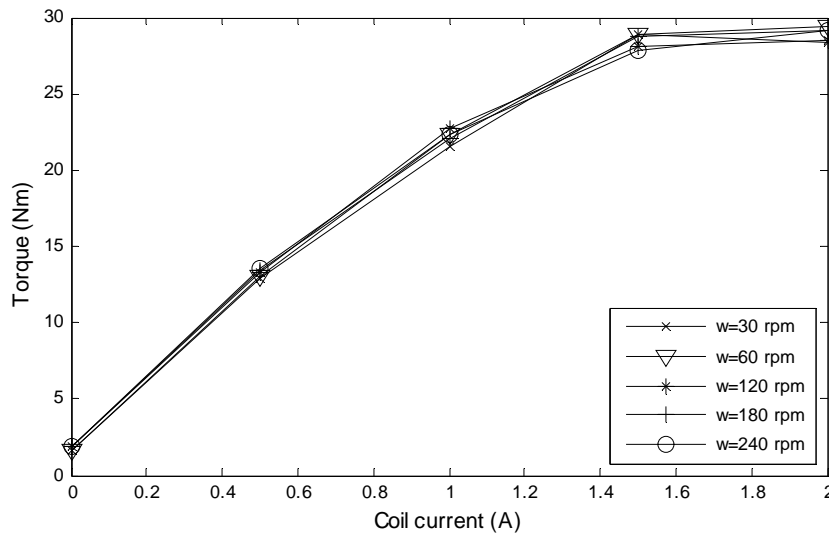


Figure 9. Total transmitted torque vs. coil current at different rotary speeds

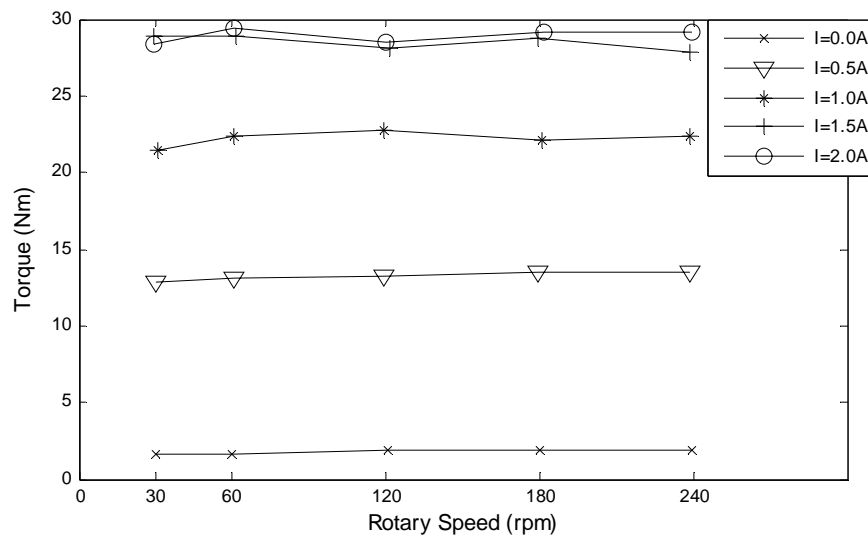


Figure 10. Total transmitted torque vs. rotary speed at different coil currents

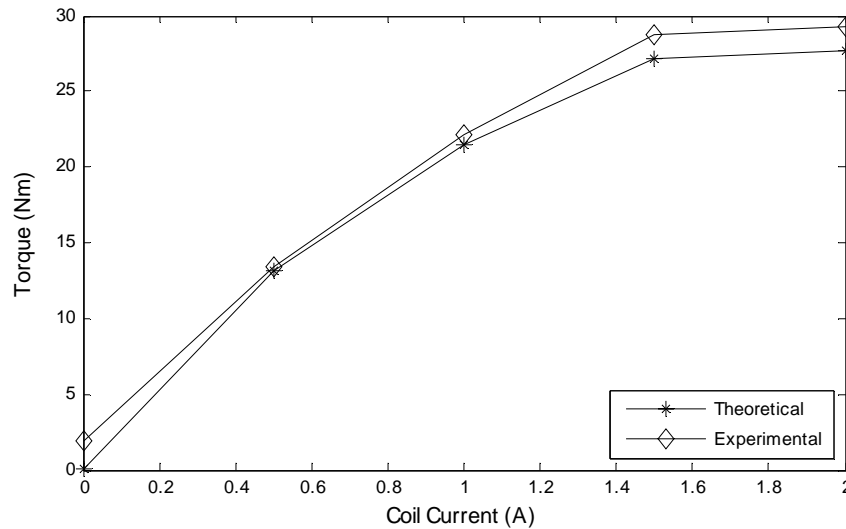


Figure 11 Experiment validation of MR pin joint performance ( $\omega=180\text{rpm}$ )

For design and control considerations, the other findings of this preliminary study can also be summarized as follows:

1. Coulomb force contributes more than 90% of the total torque of the MR pin joint. An approximate linear relationship was found between the torque and coil current before the saturation point.
2. A slight increasing trend was observed with rotary speed, although this is very small.
3. Unlike the MR damper in which the gap size is critical for its damping ability, this is of less importance in MR pin joints. However, a large plate radius will lead to a large torque output.

## 8 REFERENCES

- Carlson J. D., Leroy D. F., Holzheimer J. C., etc., (1997). Magne torheological Fluids Brake, US Patent, No. 9708853
- Fujino, Y., Soong, T.T. & Spencer Jr., B.F., (1996). Structural Control: Basic Concepts and Applications. Proc. ASCE Structures Congress XIV, Chicago, Illinois, 1996, pp. 1277-1278.
- Hiemenz G. J., Choi Y. T. & Wereley N. M., (2003). Seismic Control of Civil Structures Utilizing Semi-Active MR Braces. Computer-Aided Civil Infrastructure Engineering, Vol. 18:31-44.
- Li W. H. & Du H., (2003). Design and Experimental Evaluation of A Magnetorheological Brake. International Journal Advanced Manufacture Technology, Vol.21:508-515.
- Li, J. & Samali, B., (2003). Control of a Five Story Building Model Under Benchmark Earthquake Using SMA Actuators. Proceedings of the 5th International Conference on Motion and Vibration Control, Dec 4-8 2000, Sydney, Australia, Vol. 1:173 - 179.
- Soong, T.T., (1990). Active structural Control: Theory and Practice. Longman Scientific and Technical, Essex, England.
- Widjaja J., Samali B. & Li J., (2007). The Use of Displacement Threshold for Switching Frequency Strategy for Structural Vibration Mitigation. Journal of Mechanical Science and Technology, Vol. 21:865-869.
- Xu Y. L. & Chen B., (2008). Integrated vibration control and health monitoring of building structures using semi-active

friction dampers: Part I-methodology. Engineering Structures, 2008, in press [doi: 10.1016/ j.engstruct. 2007. 11. 013].